J. Physiol. (1975), **246**, *pp.* 55–78
With 10 *text-figures*
Printed in Great Britain

POTASSIUM RECTIFICATIONS OF THE STARFISH OOCYTE MEMBRANE AND THEIR CHANGES DURING OOCYTE MATURATION

BY *SHUN-ICHI MIYAZAKI, HARUNORI OHMORI AND SHIGETO SASAKI

From the Department of Neurophysiology, Institute of Brain Research, School of Medicine, University of Tokyo, Tokyo, Japan

(*Received 4 April 1974*)

SUMMARY

1. The current–voltage relations of the oocyte membrane of the starfish, *Asterina pectinifera*, and their changes during maturation were investigated using current-clamp and voltage-clamp techniques.

2. The resting potential of the oocyte membrane in sea water was found to be determined by the diffusion potential of K ions.

3. In the absence of Na and Ca inward currents the steady-state current–voltage relation of the oocyte membrane had inward-going K rectification at membrane potentials more negative than −65 mV and outward-going K rectification at potentials more positive than −30 mV, forming a S-shaped $I-V$ curve.

4. A negative resistance region of the steady-state $I-V$ curve was revealed with voltage-clamp technique in the potential range between −65 and −30 mV.

5. Transient K activation occurred when the membrane was brought from a resting potential of about −75 mV to potentials more positive than −20 mV, and this was immediately followed by K inactivation. Accordingly, the steady-state $I-V$ relation showed only slight outward-going rectification.

6. At the beginning of meiosis, which is signalled by break-down of the nucleus, the limiting slope conductance in the inward rectifying region of the $I-V$ curve decreased sevenfold. The cell membrane lost its selective permeability to K ions and was depolarized from −70 to between −20 and 0 mV in standard artificial sea-water. The depolarized resting potential was partly due to the relative increase in Na permeability. K conductance began to increase again within 30 min after break-down of the nucleus.

* Present address: Department of Physiology, School of Medicine, UCLA, Los Angeles, California, 90024, U.S.A.

The resting potential became gradually larger and eventually attained -70 mV in the mature egg.

7. In the mature egg, K activation upon depolarization was no longer followed by inactivation. Accordingly, the slope conductance in the outward rectifying region of the I–V curve increased.

8. The action potential was augmented at the stage of nuclear breakdown. Thereafter the maximum rate of rise decreased and the duration of the action potential shortened. These changes were caused primarily by changes in K conductance during maturation.

9. Fertilization of the egg during the maturation process did not affect the changes in the I–V relation described above, except for a transient change of the membrane permeability upon fertilization.

INTRODUCTION

Oocyte maturation and ovulation are the initial events of embryonic development. There is evidence that these processes are accompanied by changes in ionic permeabilities of the egg cell membrane. In toad eggs, the membrane resistance of the mature egg is much higher than that of the oocyte, and the selective K permeability of the membrane disappears after maturation (Maeno, 1959). The frog oocyte is predominantly permeable to K and Cl ions, whereas the ovulated, unfertilized egg is permeable to Na and Cl ions (Morrill, Rosenthal & Watson, 1966). Thus, significant changes in K conductances are expected during the process of maturation.

In the preceding paper it was demonstrated that the starfish oocyte membrane can generate a Ca- and Na-dependent action potential and that steady-state current–voltage relation formed a characteristic S-shaped I–V curve (Miyazaki, Ohmori & Sasaki, 1975). In the present study the I–V relation was further analysed with both current-clamp and voltage-clamp techniques. Special attention was given to changes in the K conductance of the egg cell membrane during maturation. In the starfish, spawning and oocyte maturation can be induced by a hormone, 1-methyladenine (Kanatani, Shirai, Nakanishi & Kurokawa, 1969; Kanatani, 1969). Use of 1-methyladenine enabled us to record electrical responses of the membrane continuously during maturation.

METHODS

The starfish *Asterina pectinifera* was used in all experiments. Most of the techniques used have been described in the preceding paper (Miyazaki *et al.* 1975). Most of the results were obtained by current-clamp method using one intracellular microelectrode. In order to obtain supporting evidences for a negative resistance region

in the steady-state $I-V$ curve and for early outward current (see Results), the voltage-clamp technique was applied by inserting two micro-electrodes into an egg in some experiments, although in many cases the insertion of two electrodes caused leak currents which resulted in a depolarized resting potential and a less marked S-shaped $I-V$ curve. The resistance of a current electrode filled with 3 M-KCl was 10–15 MΩ. Since the egg cell was a sphere (average diameter 185 μm), and since potential responses to constant current pulses recorded with two electrodes at opposite ends of the egg were the same, the condition for space clamp was satisfied. Detailed voltage-clamp technique for the egg cell membrane will be presented elsewhere (H. Okamoto, K. Takahashi & K. Yoshii, in preparation). The present technique allowed a time resolution up to 2 msec between the capacitive surge and the measurement of current.

Standard artificial sea-water (std ASW) was composed of (mM) NaCl 452, KCl 9·8, $CaCl_2$ 10·6, $MgCl_2$ 48 and Tris (buffered to pH 8·0 with HCl) 10. Since the oocyte membrane shows a Na- and Ca-dependent action potential (Miyazaki *et al.* 1975), the regenerative components were eliminated as much as possible when the $I-V$ relation was analysed. The Na component was eliminated by replacing NaCl with iso-osmolar Tris-HCl. The Ca component was suppressed by reducing Ca to one tenth of the standard concentration or by isosmotic addition of 20 mM-Co, which blocked the Ca component (Miyazaki *et al.* 1975). When Co ions were added in Na-free ASW, NaCl was replaced by isotonic urea (Urea Na-free ASW) to avoid Co-Tris complex formation (see page 355, Geduldig & Junge, 1968). Ca-free solutions were not used since they produced unstable membrane potentials and low membrane resistances. Thus, two kinds of solutions were used: 1·06 mM-Ca, Tris Na-free ASW or 20 mM-Co, Urea Na-free ASW. For more precise investigation of the $I-V$ relation with the voltage-clamp method, Ca current was minimized by adding 20 mM-Mn ions, a blocking agent of a Ca spike (Fatt & Ginsborg, 1958; Hagiwara & Nakajima, 1966), in 1·06 mM-Ca, Tris Na-free ASW. Tris Na-free was used in order to preserve the normal ionic strength of the solution as much as possible. A spectrometric observation showed that Mn ions were less complexed by Tris than Co, and that 4 mM mercaptoethanol reduced the degree of Mn-Tris complex formation. There was no significant effect of 4 mM mercaptoethanol alone on the $I-V$ relation.

Application of 1-methyladenine. 1-methyladenine (1-MA) induces 100% oocyte maturation in the starfish with a minimal effective dose of 3×10^{-7} M (Kanatani *et al.* 1969; Kanatani, 1969). Most of the results during maturation were obtained by applying 2×10^{-6} M-1-MA (Sigma) to an isolated oocyte while the recording electrode was inside the cell. In other cases, spawning and maturation of eggs were induced by 1 to 2×10^{-6} M-1-MA and the eggs were impaled subsequently.

During maturation the oocyte divides into two cells, one of which is a polar body. This meiosis occurs twice, and the number of chromosomes in a cell reduces to one half in each maturation division. The initiation of the first meiosis in isolated oocytes is signalled by the break-down of the germinal vesicle (the nucleus) and of the follicle. In our experiments (20–23° C) the break-down occurred 20–30 min after the application of 1-MA. The first polar body became visible in 60–80 min and the second polar bodies appeared about 2 hr after the application of 1-MA. The completion of the maturation process was thought to occur within about 2·5 hr of 1-MA application. Consequently, an egg bathed in 1-MA solution for more than 2·5 hr will be defined as a *mature egg*. Ovulation was induced by 1-MA in 30–40 min. In the ovulated egg the germinal vesicle has disappeared. The advance of maturation after ovulation was nearly the same as in the isolated oocyte.

RESULTS

I. Analysis of the current–voltage relation in the oocyte

Hysteresis in the transitional region of the I–V curve

Resting potentials in a Na-free condition ranged between −70 and −80 mV. Fig. 1*B* shows a steady-state current–voltage relation in the absence of an action potential (filled circles). Membrane potentials were measured at the end of current pulses of duration 3·0 sec. As in std ASW (Miyazaki *et al.* 1975), the *I–V* curve had three characteristic portions,

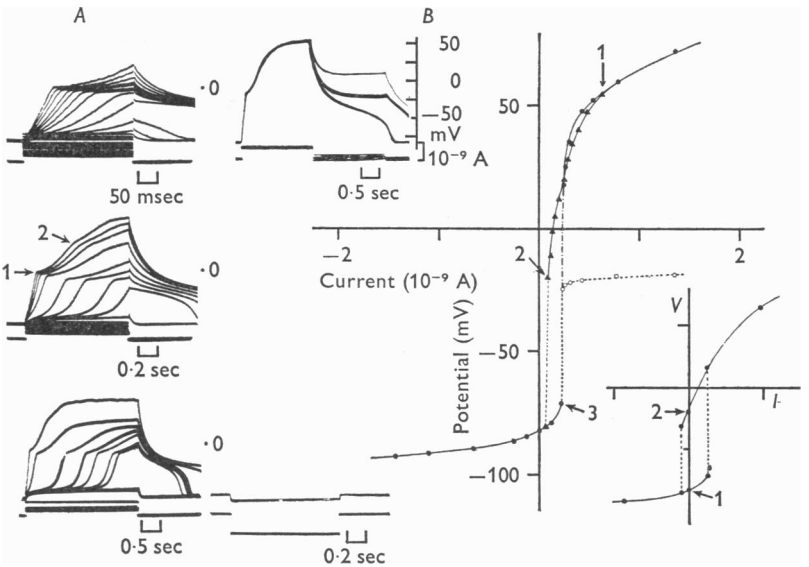

Fig. 1. *A*, electrical responses in 20 mM-Co, Urea Na-free ASW recorded with three sweep speeds to demonstrate the potential rise during depolarization. The first potential jump, the 'step' (arrow 1) and the second potential rise are clearly illustrated. There is a slight hump at +35 mV (arrow 2). The potential scale is the same as in left-hand inset of *B*, although only zero potential is indicated.

B, the *I–V* curve (filled circles) was obtained from another oocyte with current pulses of 3·0 sec. Current intensity on the abscissa and membrane potential on the ordinate. Further explanation is in the text.

inward-going rectification at membrane potentials more negative than −70 mV, outward-going rectification at potentials more positive than +20 mV and the transitional zone between the two. Fig. 1*A* was obtained from another oocyte in 20 mM-Co, Urea Na-free ASW. A potential jump occurred from the critical level of −65 mV during a depolarizing pulse, in spite of the absence of an action potential. The membrane began to

repolarize immediately after current cessation, without showing a regenerative response after the pulse (Fig. 1*A*, upper and middle records). In addition to the potential jump, there was a noticeable 'step' in the rising phase of the depolarizing response (arrow 1 in Fig. 1*A*). The step appeared at about −20 mV. The potential jump was separated into two parts: the first jump from the critical level at −65 mV to the 'step' at −20 mV and the second one from the step to the final steady level. Thus, there are two transitions in the *I–V* relation: one (dotted line in Fig. 1*B*) below and one (interrupted line) above the 'step' level. Open circles in Fig. 1*B* indicate the potential of the 'step' plotted against current intensity. The step was approximately at −20 mV, irrespective of applied currents. During the falling phase after current cessation, there was a plateau at about −20 mV.

In left-hand inset of Fig. 1*B*, the membrane was first depolarized to a large positive steady level (+55 mV, indicated by arrow 1 in the graph) by a conditioning pulse and then repolarized from that level by smaller test pulses. The potential at the end of the second pulse was plotted against current intensity (Fig. 1*B*, filled triangles). Slope resistance became larger with increasing repolarization from +55 mV and was nearly infinite at about −20 mV (arrow 2, Fig. 1*B*). In accordance with the increase in slope resistance, the time constant of a potential response became larger with increasing repolarization and a long plateau was formed at about −20 mV. With slightly smaller current, a potential jump occurred in the hyperpolarizing direction from −20 mV to a potential close to the original resting potential (dotted line in the curve of filled triangles, Fig. 1*B*). Critical current intensity for the repolarizing potential jump was $0{\cdot}8 \times 10^{-10}$ A (arrow 2, Fig. 1*B*), whereas the valve for the depolarizing potential jump was $2{\cdot}2 \times 10^{-10}$A (arrow 3). Thus, a hysteresis exists between these two portions of the *I–V* curve.

The remarkable S-shaped *I–V* curve shown in Fig. 1*B* may allow two stable states of membrane potential. Since the *I–V* curve during repolarization (filled triangles) is very close to the potential axis at the point indicated by arrow 2, a slight residual inward current or a slight leak current would keep the membrane potential at this potential level. In the right-hand inset of Fig. 1*B*, two resting potentials are illustrated schematically: a hyperpolarized one (1) and a depolarized one (2). In fact, there was an oocyte which showed two resting potentials (see description about Fig. 9 in the preceding paper).

Voltage-clamp analysis of the I–V relation

The hysteresis shown in Fig. 1*B* suggests the existence of a negative slope region in the steady-state *I–V* curve, as described in the tunicate

embryo (Miyazaki, Takahashi, Tsuda & Yoshii, 1974*b*). Since the negative resistance can not easily be demonstrated under the current-clamp condition, the voltage-clamp technique was used. Fig. 2*A* illustrates membrane currents associated with rectangular depolarizations in std ASW (inward current upward). Fig. 2*B* shows early currents with faster time base. The peak of the inward current, presumed to be due to Na and Ca influx, was plotted against membrane potential in Fig. 2*C* (open circles). Note that the axes are reversed from their usual orientation. The same data presented

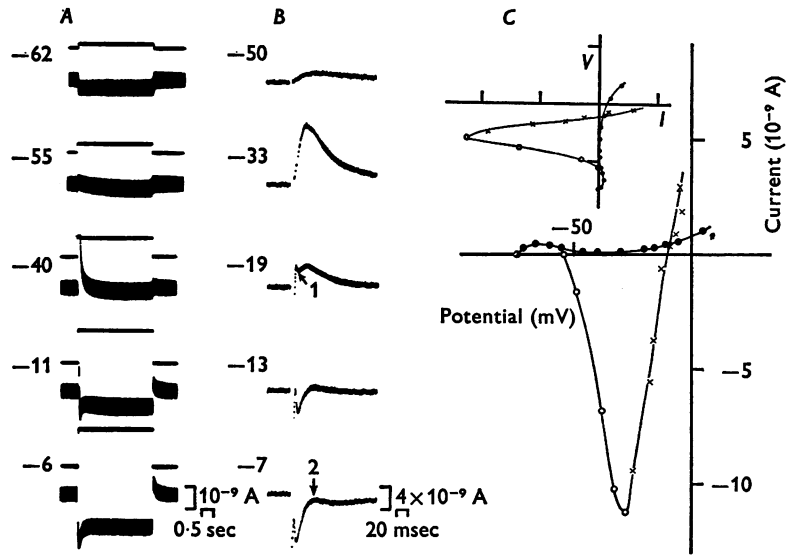

Fig. 2. *A*, membrane current (lower trace) associated with rectangular depolarization (upper trace) in std ASW with slow time base. Holding potential is −74 mV and the clamped potential level is indicated by the figure in each record. Inward current is upward.

B, membrane current with fast time base.

C, *I*–*V* relation at the steady state (filled circle) and at the peak of inward current (open circle). Curve through cross symbols is explained in the text. Outward current: positive. Note the reversed axes (membrane potential on the abscissa and membrane current on the ordinate). Inset is a schematic illustration of the same *I*–*V* curves by usual *I*–*V* plot used in other Figures.

with the potential axis as the ordinate are schematically shown in inset of Fig. 2*C*. The inward current first appeared with a potential step to −55 mV and was maximal at −25 mV. With depolarization to potentials more positive than −20 mV, the initial part of inward current seemed to be lowered by a rapid outward surge (arrow 1), as shown in the records of −19 and −13 mV in Fig. 2*B*. With depolarization to −7 mV, the inwardly directed component still remained (arrow 2 in Fig. 2*B*) after the rapid surge, though the membrane current was outward throughout

the potential pulse. The current intensity at the reduced peak of inward current or during the inwardly directed component (arrow 2) was plotted with cross symbols in Fig. 2*C*. The apparent reversal potential of the inward current component was about −10 mV. However, this value is likely to be more negative than the actual reversal point, due to interference from early outward current. The appearance of the transient outward current corresponds to the 'notch' seen in the rising phase of the action potential (see arrow 1 in Fig. 2*C* of the preceding paper, Miyazaki *et al.* 1975), and the low reversal potential corresponds to the low peak of the action potential (no overshoot above 0 mV). The peak is thought to be determined by the balance between Ca and Na inward currents and the outward current.

The membrane current at steady state was always outward, being measured at the end of the depolarizing command pulse of 3·3 sec duration (Fig. 2*C*, filled circles). The *I–V* curve had a negative slope in the potential range between −65 and −30 mV. Since both Na and Ca ions are present in std ASW, the observed negative slope region might be due to residual inward currents of Na and Ca. To reduce the inward current as much as possible, the solution 20 mM-Mn, 1·06 mM-Ca, Tris Na-free ASW with 4 mM mercaptoethanol was used (see Methods). Only a slight inward current could be seen just after the membrane potential was changed to the level at which the inward current was large in std ASW (Fig. 3*A*, −38 mV). The membrane current was nearly rectangular during the voltage clamp at levels up to −30 mV (see upper record of inset in Fig. 3*B*). In Fig. 3*B* membrane current obtained with the voltage clamp was plotted on the abscissa and membrane potential on the ordinate. In the potential range between −65 and −30 mV the current intensity at steady-state was progressively less with more depolarization, as shown in curve 2 of Fig. 3*B* (filled triangles). Thus, the negative slope in the steady-state *I–V* curve was confirmed. With depolarization to potentials more positive than −30 mV the slope of the *I–V* curve (2 in Fig. 3*B*) became positive and coincided with curve 1 (filled circles) obtained with the current clamp.

As shown in the lowest two records of Fig. 3*A*, a rapid outward surge appeared immediately after the change of the membrane potential to levels more positive than about −20 mV. It decreased markedly within 0·5 sec and then slowly attained a steady value. The transient peak of outward current (see lower record of inset, Fig. 3*B*) was plotted against membrane potential with open triangles (Fig. 3*B*). The *I–V* relation for the 'potential step' with constant current pulse (see Fig. 1) was also plotted with open circles in Fig. 3*B*. The results show a marked increase in the transient outward current at about −15 mV, a level identical to that of the 'step' in the rising phase of the depolarization by the constant

current pulse. This transient phenomenon is considered as activation and inactivation processes of outward current. The second potential jump (from the 'step') in the depolarizing response to constant current (Fig. 1) is due to this inactivation which shifts the $I-V$ relation from curve 3 to 2 in Fig. 3*B*.

In summary, the steady-state $I-V$ relation has inward-going rectification below -65 mV, outward-going rectification above -30 mV and a negative resistance region between them. In addition, a transient increase of outward current occurs above -20 mV.

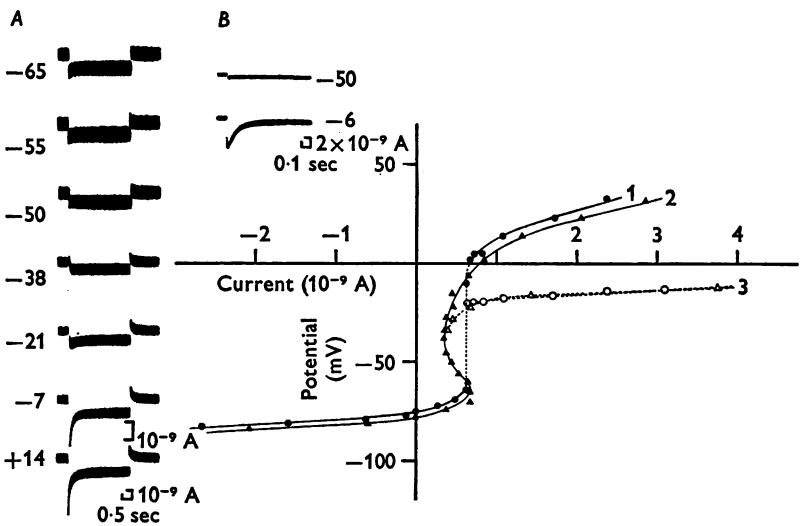

Fig. 3. *A*, membrane current during the voltage clamp in 20 mM-Mn, 1·06 mM-Ca, Tris Na-free ASW (merceptoethanol, 4 mM). Holding potential -77 mV. *B*, membrane current obtained with the voltage clamp is plotted on the abscissa for easier comparison with the current-clamp results. Curve 1 (●) and 2 (▲) are steady-state $I-V$ curves with the current- and voltage-clamp technique respectively. In curve 3 (dotted line), open triangles indicate the $I-V$ curve at the peak of transient outward current, and open circles indicate the $I-V$ relation at the 'step' in the rising phase of depolarizing response to constant current pulse.

Effects of K ions on the I–V curve

The resting potential of the oocyte membrane in Na-free ASW changed 57 mV for tenfold change in external K concentration over the range from 10 to 100 mM (Fig. 4*C*). This indicates that the resting potential in Na-free ASW is defined by the K diffusion potential across the membrane. In Fig. 4*A*, K concentration was increased by four times (39 mM) or decreased to one fourth (2·5 mM) in 1·06 mM-Ca, Tris Na-free ASW. The resting

potential shift of 34 mV (39 mM-K) or −30 mV (2·5 mM-K) was accompanied by a shift in the hyperpolarizing portion of the *I–V* curve. The limiting slope resistances in this portion decreased with increasing K concentration; 6·3 MΩ in 2·5 mM-K, 4·7 MΩ in 9·8 mM-K and 3·0 MΩ in 39 mM-K solution. *I–V* curves in higher K (98, 196 and 392 mM) of Na-free ASW are illustrated in Fig. 4*B*. The resting potential was about

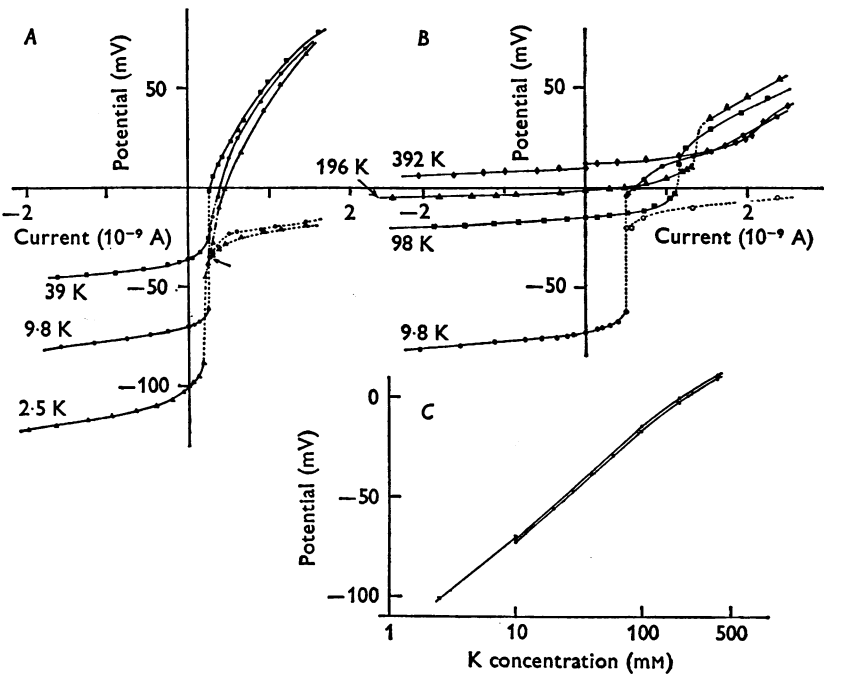

Fig. 4. *A*, *I–V* curves obtained with the current clamp at different concentration of K ions in 1·06 mM-Ca, Tris Na-free ASW. The pulse duration was 2·8 sec. Potential measurement was the same as in Fig. 1*B*.

B, *I–V* curves at high external K concentration in a Na-free condition. The pulse duration was 2·8–3·0 sec.

C, the relationship between membrane potential and the logarithm of external K concentration, obtained from three oocytes in Na-free ASW or in 1·06 Ca, Na-free ASW.

0 mV in 196 mM-K solution so that the internal K concentration is estimated to be about 200 mM. This value is nearly consistent with the reported value in the eggs of another kind of starfish, *Asterias forbesi* (Tyler, Monroy, Kao & Grundfest, 1956). The average resting potential in std ASW was nearly identical to the calculated K equilibrium potential (−76·0 mV). Accordingly, the oocyte membrane has selective K permeability in the resting state in std ASW.

The critical potential level for the depolarizing potential jump was usually about 10 mV more positive than the resting potential. This relation between the critical level and the resting potential was maintained even when the resting potential was shifted by changes in external K concentration (Fig. 4*A*). In addition to this vertical shift of the *I–V* curve, there was also a horizontal shift: the higher the K concentration, the larger the amount of current needed to produce a constant amount of potential change. This was evident at higher K concentration (Fig. 4*B*). Thus, the critical level for the potential jump is dependent upon the electrochemical potential of K ions. That is the case for conductance which is the basis of anomalous rectification in other excitable membranes (see Discussion for references). The negative resistance region of the steady-state *I–V* curve can be explained by the marked decrease of K chord conductance with increasing depolarization. The negative resistance causes the initiation of the potential jump in response to constant current (Fig. 1*A*). This phenomenon has been described in the eel electroplaque (Nakamura, Nakajima & Grundfest, 1965) and in the gastrula embryo of the tunicate (Miyazaki *et al.* 1974*b*).

The outward rectifying region above the potential jump was relatively less affected by changes in external K concentration (Fig. 4*A*). Outward rectifying current is probably carried by K ions, because these are the main intracellular permeant cations (200 mM, see above). The possibility that Cl ions might be the charge carrier of the outward current was excluded when no change in the *I–V* curve was found after complete replacement of external Cl with methansulphonate. The outward rectifying region seems to be mainly dependent upon internal K concentration rather than external K. For decisive identification of K for the outward-going rectification, further study will be necessary to show that its reversal potential is consistent with the K equilibrium potential and that it changes with external K concentration.

If we consider the outward current to be K outflux, the transient phenomenon appearing at -20 mV (Fig. 3) can be defined as K activation followed by inactivation. The critical activation level was 15 mV more negative in one-tenth Ca (1·06 mM) solution (arrow in 9·8 K, Fig. 4*A*), and it was nearly the same in 2·5 K, 1·06 mM-Ca solution (Fig. 4*A*). The transient K activation was not observed in high K solution (Fig. 4*A*, 39 K and Fig. 4*B*, 98, 196 and 392 K) in which the resting potential was more positive than the K activation level. The transient increase in K conductance is probably inactivated by a maintained depolarization, as shown in delayed rectification of frog's skeletal muscle in high K media (Nakajima, Iwasaki & Obata, 1962). TEA (tetraethylammonium) ions are known to selectively block delayed rectification in excitable membranes (Tasaki &

Hagiwara, 1957; Armstrong & Binstock, 1965; Hille, 1967). In the starfish oocyte, neither transient K activation nor the outward-going rectification over the positive potential range was affected by externally applied 100 mM-TEA (substituted for 100 mM-Na) in std ASW even after 5 hr application.

II. Changes in the I–V relation during maturation induced by 1-MA

For convenience, the maturation process was divided into the early and the late phase. The early phase consisted of the first 30 min after application of 1-MA. The end of this phase usually coincided with break-down of the germinal vesicle (see Methods). The late phase began 30 min after 1-MA application and ended 2–2·5 hr later, when the maturation process was completed.

Resting potential and I–V relation at the early phase of maturation

In order to examine the changes in K conductance exclusively, Na-free ASW was used. The maturation process in Na-free ASW was similar to that in std ASW. Fig. 5*A* illustrates a resting potential shift and a change in the membrane resistance for hyperpolarizing current during the early phase of maturation. 2×10^{-6} M-1-MA was applied at the time indicated by the arrow. Seven to 8 min later, the response to the hyperpolarizing current pulses of constant intensity gradually increased, and the membrane was depolarized from the original resting potential of -71 mV. The depolarization induced repetitive action potentials, which had extremely long falling phases. In this experiment the membrane potential reached a steady level of -38 mV 20 min after addition of 1-MA. Hyperpolarization beyond -70 mV induced a regenerative response after termination of the pulse (see Fig. 5*C*, lower record).

The *I–V* relation of this egg membrane at the end of the early phase was plotted in Fig. 5*B* (curve 2, filled circles) and was compared with that of the same oocyte before 1-MA application (curve 1, open circles). The inward-going rectification below -70 mV was still observed, but the limiting slope resistance in the hypopolarizing direction had become eight times larger than that in the immature oocyte. The slope resistance in the outwardly rectifying region was also larger in curve 2 (at potentials less positive than $+65$ mV). These changes in slope resistance combined to produce an *I–V* curve with a less pronounced S-shape. The hysteresis shown in Fig. 1*B* became less marked, and the negative resistance region was rarely observed (Fig. 8*C*, curve 1). Therefore, the potential jump evoked by constant current pulses (Fig. 1*A*) was rarely observed by the end of the early maturation phase. The change in effective surface area of the egg was negligible during maturation, for a total membrane capacity

which is considered to indicate a relative value of the effective surface area was in the range 0·9 and $1{\cdot}2 \times 10^{-9}$ F in both the oocyte and the egg during maturation. Therefore, the changes in slope resistance described above are based upon changes in specific membrane resistance.

In std ASW the decrease in resting potential and the increase in limiting slope resistance in the hyperpolarizing direction were also found at the early phase of maturation. However, the final steady level of the resting potential was between −20 and 0 mV, which was less negative than in

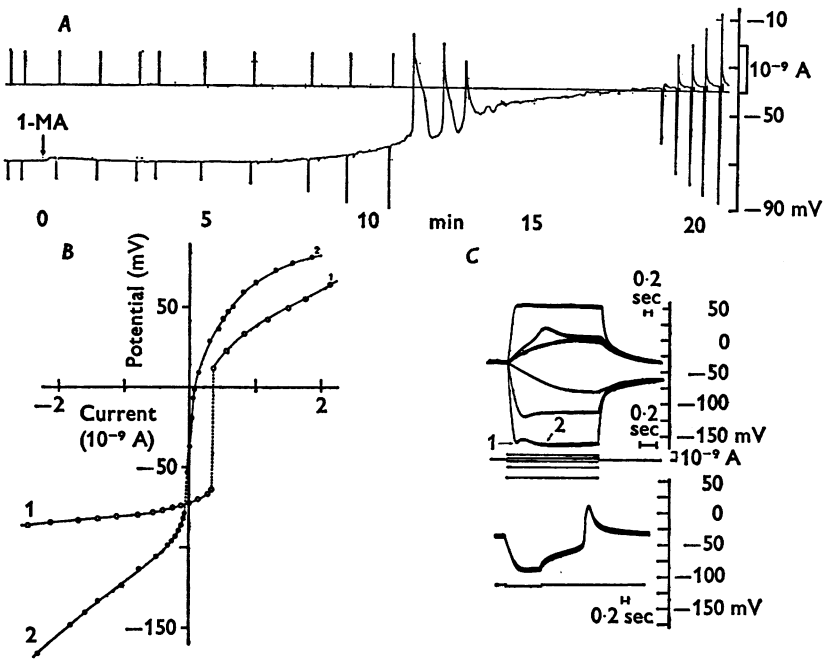

Fig. 5. *A*, the resting potential shift and the change in membrane resistance for hyperpolarizing current during the early phase of maturation. Upper trace shows current, lower trace shows membrane potential.

B, *I–V* relations in the oocyte (curve 1, open circles) and in the egg 30 min after 1-MA application (curve 2, filled circles). Dotted line indicates the potential range at which steady potential could not be obtained at the end of the current pulse.

C, electrical responses in the egg at the end of the early phase of maturation. In upper record, sweep speed is different in depolarizing and hyperpolarizing responses. There was an undershoot (arrow 1) followed by an increasing hyperpolarization (arrow 2), when the membrane was hyperpolarized to a potential more negative than −160 mV. These responses may suggest activation followed by inactivation of K current, similar to that seen upon depolarization over −20 mV.

All records were obtained from the same egg in Na-free ASW. Detailed explanations are in the text.

Na-free ASW. The increased slope resistance was about half that in Na-free ASW. These are probably due to the relative increase of Na conductance. As in the oocyte, Cl removal from external solution at the end of the early maturation phase did not affect either the resting potential or the $I-V$ curve.

Changes in the $I-V$ relation in the late phase of maturation

After break-down of the germinal vesicle, the $I-V$-relation in an egg changed progressively in the manner shown in Fig. 6 (curves 3 to 7). The significant changes were as follows:

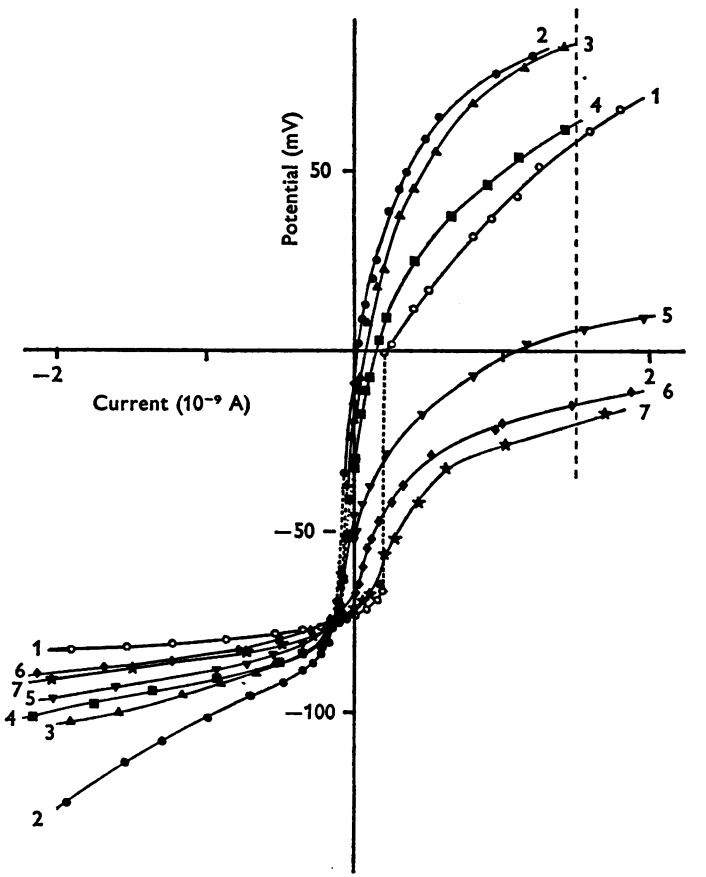

Fig. 6. Changes of the $I-V$ relation in std ASW during maturation induced by 1-MA. Curves were obtained in one egg: curve 1, oocyte; curve 2, 30 min after 1-MA application; curve 3, 1 hr; curve 4, 2·3 hr; curve 5, 3·2 hr; curve 6, 4 hr; curve 7, 5 hr. Membrane potential was measured at the end of current pulses of about 3 sec. Membrane potential corresponding to current $I = 1{\cdot}5 \times 10^{-9}$ A (dashed line) is plotted in Fig. 7*B* against time after 1-MA application.

(1) The limiting slope resistance of the inward rectifying region decreased within 1 hr after 1-MA application (from curve 2 to 3) and became similar to the value in the immature oocyte (Fig. 7*A*). In association with the increase in K conductance, the resting potential became gradually hyperpolarized. The limiting slope resistance of the inward rectifying region is plotted against time after 1-MA application in Fig. 7*A*.

(2) The slope of the *I–V* curve in the outward rectifying region decreased, and the *I–V* curves in this region shifted in the negative direction. In order to illustrate these changes more clearly, the membrane potential corresponding to a current pulse of $1{\cdot}5 \times 10^{-9}$ A is plotted also against time after 1-MA application in Fig. 7*B*.

From the comparison of Fig. 7*A* with *B* it is evident that the decrease in limiting slope resistance (event 1) and the shift of the outward rectifying region in the negative direction (event 2) did not occur at the same time: event 1 was prominent in the first 1–1·5 hr while event 2 occurred rather abruptly at 2·5 hr after 1-MA application. The time courses of the two events were nearly the same in Tris Na-free ASW and Urea Na-free ASW with Co as in std ASW (Fig. 7*A*, *B*), and they were independent of the presence of 1-MA after break-down of the germinal vesicle. Even fertilization did not affect the time course of the events (see below).

There is a possibility that these events might be the result of increased leak current due to electrode impalement lasting more than 5 hr or that the maturation process might be affected by the frequent current application. To eliminate these possibilities, eggs were impaled at fixed times after 1-MA application (open triangles in Fig. 7*A* and *B*). The results indicate that the long-lasting recording did not affect the development of the above mentioned events 1 and 2.

There were some eggs which matured spontaneously without 1-MA application. In such eggs, events 1 and 2 were also observed, although the early phase could not be carefully monitored because of the uncertainty in the time of the initiation of spontaneous maturation.

K activation and inactivation during maturation

In order to clarify the nature of the enhanced outward-going rectification in the late phase of maturation, the *I–V* relation was examined after elimination of the action potential (Fig. 8). As in the oocyte, the egg at the early phase showed a transient increase of K conductance with depolarizations to potentials more positive than -20 mV. This caused the 'step' in the rising phase of the depolarizing response to constant current (arrow in Fig. 8*A*1). The transient outward current is shown in the voltage-clamp records of Fig. 8*B*1 (lower two records), and its peak was plotted with open circles in Fig. 8*C*. Since the K activation was immediately followed by inactivation, the final steady-state *I–V* relation had only slight outward-going rectification in the potential range from -20 to $+30$ mV, as shown in Fig. 8*C* curve 1 (filled circles).

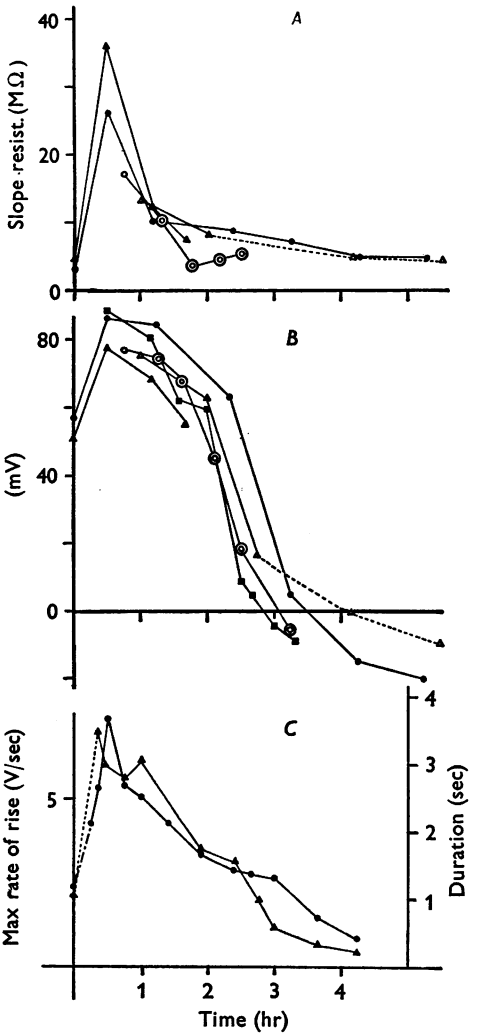

Fig. 7. *A*, the limiting slope resistance in the hyperpolarizing region of the *I–V* curve, plotted against time after 1-MA application.

B, changes in potential corresponding to depolarizing current of $1{\cdot}5 \times 10^{-9}$ A in the *I–V* curve (see Fig. 6 for measurement).

Symbols are common in *A* and *B*: ●, egg illustrated in Fig. 6 (std ASW); ▲, another egg in Na-free ASW; △, three eggs impaled at various times after 1-MA application (Na-free). △ symbols are connected with a continuous line (one egg) and an interrupted line (two eggs). Symbols ○ and ◎ were obtained before and after fertilization, respectively, in an egg used for Fig. 9*B* (std ASW). The symbol ■ in *B* indicates an egg which showed potential responses in Fig. 8*A* (10 mM-Co, Urea Na-free ASW).

C, changes in the maximum rate of rise (●) and the duration (▲) of the action potential in std ASW. The duration was defined by the time between rising and falling phase measured at the critical membrane potential for the action potential.

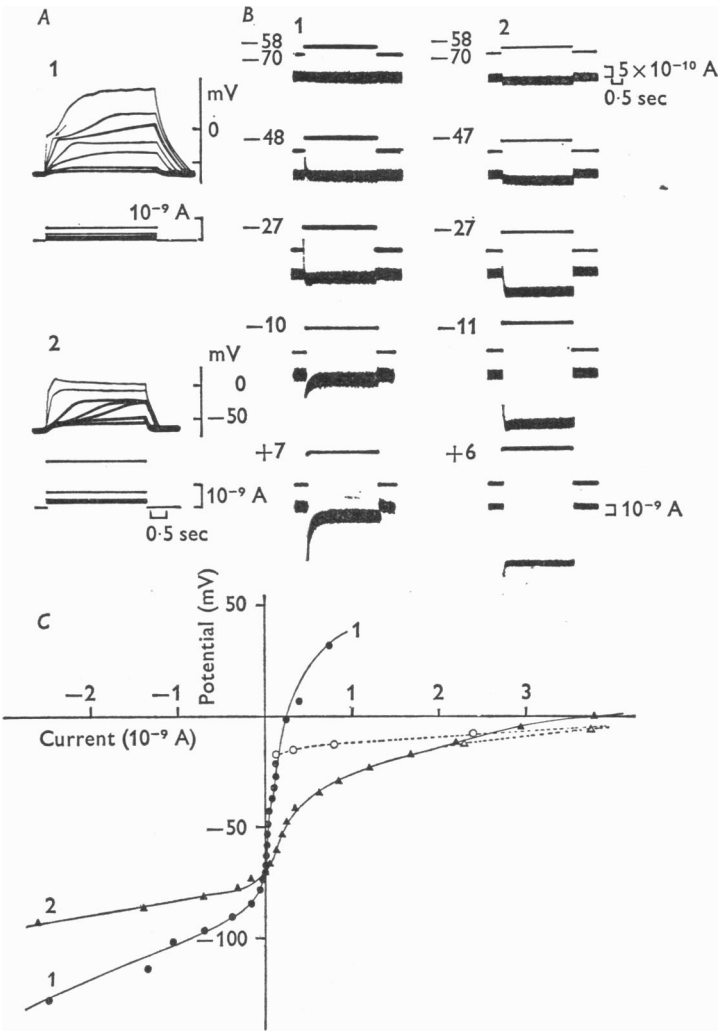

Fig. 8. *A*, potential responses to depolarizing currents in 10 mM-Co, Urea Na-free ASW: 1, an egg at the early phase of maturation; 2, a mature egg. 30 min and 3·5 hr after 1-MA application, respectively. The membrane potential was held at −72 mV by conditioning DC current.

B, membrane currents under the voltage clamp in 20 mM-Mn, 1·06 mM-Ca, Tris Na-free ASW with 4 mM mercaptoethanol. 1, an egg at the end of the early phase of maturation. 2, a mature egg at 6 hr after 1-MA application.

C, steady-state *I–V* relation at the end of potential step of 3 sec (filled symbol, continuous line) and transient *I–V* curve at the peak of the early outward current (open symbol, interrupted line). Circles and triangles correspond to voltage-clamp records *B*1 and *B*2, respectively.

In the mature egg, the amount of steady-state outward current observed with the voltage clamp was larger than in the egg of the early phase, and the difference was larger with increasing depolarization (compare curve 2 with 1 in Fig. 8*C*). The outward current was nearly rectangular at the potential range from −70 to −10 mV, although a slight residual inward current was sometimes observed just after the potential change (Fig. 8*B* 2, −27 mV). A rapid outward surge was seen at potentials more positive than −10 mV (Fig. 8*B* 2, lowest record). However, in contrast to the records at the early phase of maturation, most of the outward current was not inactivated (compare Fig. 8*B* 2 with *B* 1, lowest two records). The region of the steady-state *I–V* curve above −20 mV in the mature egg (Fig. 8*C*, curve 2, filled triangles) almost coincided with the 'transient *I–V* curve' at the peak of the early outward current in the egg of the early phase (Fig. 8*C*, open circles). Since the K activation was not followed by inactivation in the mature egg, the depolarizing response to constant current became steady at the potential level where the 'step' appeared in the egg of the early phase (compare Fig. 8*A* 2 with *A* 1). In conclusion, the enhancement of outward-going rectification at the late phase of maturation is due mainly to the disappearance of the K inactivation.

Changes in the action potential during maturation

The action potential in the mature egg membrane was both Ca- and Na-dependent, as in the oocyte (not shown here). Fig. 7*C* indicates changes in action potential parameters of an egg after 1-MA application. Since the resting potential in std ASW was different at each phase, the membrane potential was held at the same level as in the oocyte (−70 mV) with DC current, before action potentials were evoked. Values of the maximum rate of rise and the duration of the action potential were maximal at about 30 min after 1-MA application. This coincided with the least pronounced outward-going rectification (Fig. 6, curve 2) and suggests that the reduction of K outward current causes the apparent increase of the inward-directed current. Changes in the maximum rate of rise and the duration at the late phase of maturation also coincided with the change in the *I–V* relation; i.e. the increase of K outward current mainly due to the disappearance of K inactivation.

I–V relation after fertilization

The starfish egg is fertilizable at any stage after break-down of the germinal vesicle. The transient potential change at the time of fertilization, the so-called activation potential, was observed (Fig. 9*A*), similar to that found in eggs of another starfish *Asterias forbesi* (Tyler *et al.* 1956). The membrane conductance increased fivefold at the peak of the activation

potential (+9 mV). Within 10 to 20 min after fertilization, the membrane conductance still remained larger than before insemination and the $I-V$ curve was almost linear over the potential range from −45 to +35 mV as shown in curve 2 (filled circles) of Fig. 9*B*. The changes in the $I-V$ relation occurring more than 20 min after fertilization were not dependent on time after fertilization but upon time after 1-MA application (Fig. 9*B*).

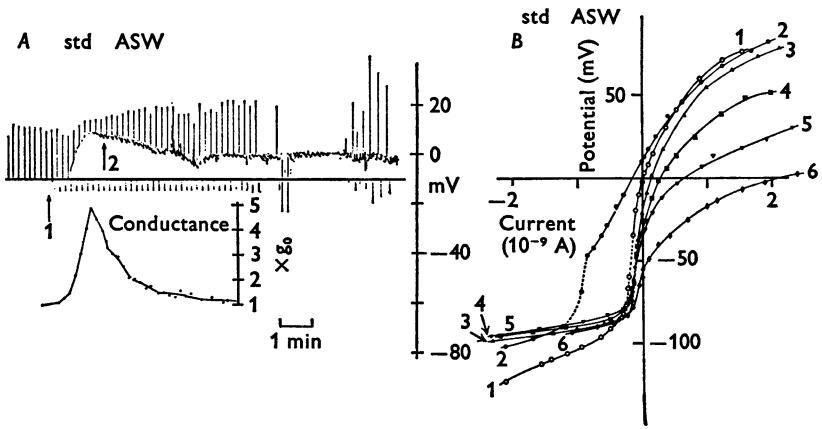

Fig. 9. *A*, activation potential upon fertilization in std ASW. A drop of sperm suspension was applied to the bath at the time indicated by arrow 1. The fertilization membrane became visible at arrow 2. Since the $I-V$ curve was almost linear in the potential range of the activation potential (see curves 1 and 2 in *B*), potential responses to successive pulses indicate the change in membrane conductance, which is expressed in multiples of that before fertilization (lower trace, same time base).

B, changes in the $I-V$ relation after fertilization in std ASW (current-clamp records): curve 1, unfertilized egg 45 min after 1-MA application; curve 2, fertilized egg 15 min after fertilization (1 hr and 15 min after 1-MA); curve 3, 45 min after fertilization; curve 4, 1 hr and 5 min; curve 5, 1 hr and 20 min; curve 6, 2 hr and 10 min. These changes are illustrated by double circles in Fig. 7*A* and *B*. When curve 5 was recorded, the other eggs in the bath began to cleave into two blastomeres, but the penetrated egg did not cleave during successive application of the current pulses.

This is clearly demonstrated in Fig. 7*A* and *B* where double circles indicate values obtained from the fertilized egg. The time courses of changes for both the inward and the outward rectifying region were exactly identical to those in unfertilized eggs.

In sea urchin eggs the membrane is hyperpolarized from −50 to −60 mV within at most 25 min of insemination, as a result of a permeability increase to K ions (Steinhardt, Lundin & Mazia, 1971; Steinhardt, Shen & Mazia, 1972; Ito & Yoshioka, 1972, 1973). Hyperpolarization after fertilization was much slower in the *Asterina* eggs used in the present study. The discrepancy may be due to the difference of species or of maturation stage at the time of fertilization.

I–V relation in cleaved eggs

Cleavage occurs 1 to 1·5 hr after fertilization. When a fertilized egg began to cleave while the electrode was inside, the electrode invariably came out of the cell. Then an egg was impaled through the fertilization membrane after cleavage. A good impalement was quite difficult and was almost impossible after 64-cell stage, because each blastomere becomes smaller at each cell division. Only a few successful penetrations were obtained, and the examples of the fertilized, uncleaved egg at 3 hr after 1-MA application (curve 1), the 16-cell embryo (curve 2) and the 32-cell embryo (curve 3) are illustrated in Fig. 10*A*. The results seem to indicate that the

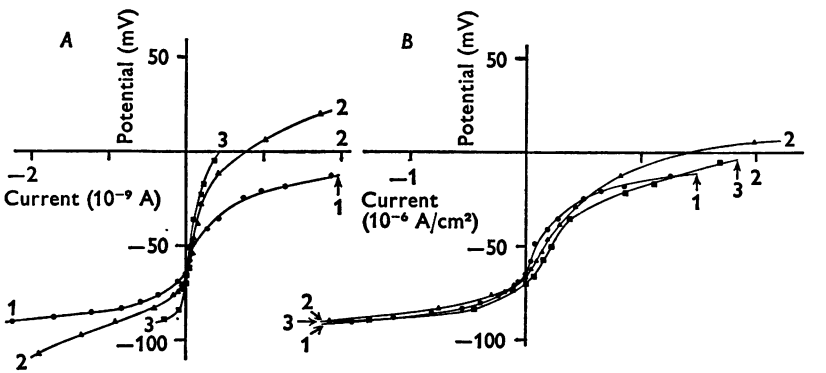

Fig. 10. *A*, *I–V* curves in the fertilized, uncleaved egg 3 hr after 1-MA application (curve 1), in the 16-cell embryo (curve 2) and the 32-cell embryo (curve 3). The contribution of the fertilization membrane was neglected, for there was no potential difference across this membrane, nor could a potential be developed across it with usual current pulses.

B, *I–V* curves normalized in terms of unit membrane area. Since the specific membrane capacity was found to be 1·0 μF/cm² in uncleaved eggs, current intensity can be expressed by A/cm². Further description is in the text.

slope resistance over the whole range of membrane potentials is larger at more advanced stages. The total membrane capacity was 1·49, 0·54 and $0{\cdot}20 \times 10^{-9}$ F for the cells illustrated in curves 1, 2 and 3, respectively. Assuming that the membrane capacity per unit area is constant, the total capacity indicates the relative value of the effective surface area of the penetrated blastomere. In Fig. 10*B* curves 2 and 3 were compared with curve 1, by multiplying the current intensity by 1·49/0·54 or 1·49/0·20 to normalize the change of the effective surface area. Three curves then became similar. Therefore, the *I–V* relation, expressed in terms of the unit membrane area, does not change appreciably after cleavage.

The effective surface area of the penetrated cell decreases at each cell division. In starfish *Asterias forbesi* embryo, it has been reported that there is no electrical communication between cells from 2-cell to 16-cell stage (Ashman, Kanno & Loewenstein, 1964; Tupper, Saunders & Edwards, 1970). In *Asterina* embryo, the electrical coupling seems to be quite weak.

DISCUSSION

K conductance in the oocyte membrane. The steady-state $I-V$ curve in the starfish oocyte membrane includes both inward- and outward-going rectification, resulting in an S-shaped curve. Between the two rectifying regions of the curve a transitional region of negative resistance is formed. The S-shaped $I-V$ curve was considered to be based on potential-dependent K conductance of the membrane. These characteristics are identical with those in the gastrula embryo of the tunicate (Miyazaki *et al.* 1974*b*).

The inward-going rectification in the frog skeletal muscle fibre has been described as 'anomalous rectification' of K conductance (Katz, 1949; Hodgkin & Horowicz, 1959; Nakajima *et al.* 1962; Adrian & Freygang, 1962). It has also been observed in cardiac Purkinje fibres (Hutter & Noble, 1960; Carmeliet, 1961; Trautwein & Kassebaum, 1961; Hall, Hutter & Noble, 1963). K inactivation described in eel electroplaques (Grundfest, 1961, 1966; Nakamura *et al.* 1965; Bennett & Grundfest, 1966), lobster muscle fibres (Reuben, Werman & Grundfest, 1961) and in supramedullary neurones of a puffer fish (Nakajima & Kusano, 1966; Nakajima, 1966) is also inward-going rectification. The K conductance which is the basis of anomalous rectification does not depend upon the membrane potential but rather upon the K electrochemical potential, and it is abolished by replacement of external K with Rb or Cs ions (Hall & Noble, 1963; Hall *et al.* 1963; Noble, 1965; Nakamura *et al.* 1965; Bennett & Grundfest, 1966). The inward-going rectification found in the gastrula embryo of the tunicate was shown to have these two characteristics (Miyazaki *et al.* 1974*b*). In the starfish oocyte the dependence of the inward-going rectification upon the K electrochemical potential was confirmed (see Fig. 4). The recent study of the starfish *Nordora punciformis* oocyte also demonstrates the interaction of Rb and Cs ions with K in the inward rectifying membrane (Hagiwara & Takahashi, 1974). Thus, the inward-going K rectification observed in the oocyte or in the embryo is considered to be the same as that found in other excitable membranes. Another feature of the starfish oocyte membrane is the transient K activation at membrane potential more positive than -20 mV. The transient increase in outward current occurred within 10 msec after abrupt depolarization and preceded the transient inward current carried by Na

and Ca ions (see voltage-clamp records in Figs. 2 and 3). Early K current, which is distinguishable from delayed rectification, has also been observed in *Onchidium* nerve cell (Hagiwara, Kusano & Saito, 1961).

K conductance during oocyte maturation. At the early phase of maturation, within 30 min after 1-MA application, both inward- and outward-going rectification became less marked. The reduction of the limiting slope conductance in the inward rectifying region was especially significant. In association with this, the resting potential shifted to a depolarized level far from the K equilibrium potential. These results suggest that the membrane loses its selective permeability to K ions. The disappearance of K selectivity of the egg membrane has also been reported in the amphibian mature egg after artificial ovulation (Maeno, 1959; Morrill *et al.* 1966).

The K conductance in the inward rectifying region of the $I-V$ curve reached a minimum at the initiation of the first meiosis. Within 30 min after break-down of the germinal vesicle the K conductance began to increase again. On the other hand, in the tunicate embryo the K conductance in the inward rectifying region remained extremely low in the egg which is ready for fertilization, and it began to increase at the two-cell stage after fertilization (Miyazaki, Takahashi & Tsuda, 1974*a*). In the tunicate, however, the egg just before fertilization stays at the metaphase of the first meiosis and the later advance of maturation, such as appearance of the polar body, is triggered only after fertilization (Conklin, 1905). Therefore, the changes of the K conductance in the inward rectifying region during maturation seem to be common to both starfish and tunicate.

The striking difference in the developmental changes of K conductance between the tunicate and the starfish occurs with the augmentation of outward-going rectification due to the disappearance of K inactivation during the late phase of maturation in the starfish egg. The phenomenon occurred rather abruptly 2·5 hr after 1-MA application, roughly at the time when the second polar bodies were formed. In the tunicate delayed rectification appeared at the late stage of the gastrula embryo and is established in differentiated muscle fibres (Takahashi, Miyazaki & Kidokoro, 1971; Y. Kidokoro, S. Miyazaki, K. Takahashi & K. Tsuda, in preparation). Development of delayed rectification was thought to have a biological significance of shortening action potentials in excitable cells (Miyazaki, Takahashi & Tsuda, 1972; Y. Kidokoro, S. Miyazaki, K. Takahashi & K. Tsuda, in preparation). In the starfish the increase in outward K current appears at early developmental stage such as the mature egg or the cleaved egg before 32-cell stage. The progressive change in outward-going rectification may indicate the development of delayed rectification as in the tunicate embryo. However, in the mature egg of the starfish, the 'delayed' increase of the K outward current could not be

revealed, even by the voltage-clamp technique, although the slope resistance in the outward rectifying region was markedly reduced. Outward current was nearly rectangular during the voltage clamp at potentials between -70 and -10 mV. 100 mM-TEA did not affect the outward-going K rectification in the mature egg, at least when externally applied.

We have no information about the role of outward-going K rectification in the mature egg. But the S-shaped $I-V$ curve seems to be a basic property of the egg plasma membrane, including the undifferentiated embryonic cell membrane. Quantitative differences in membrane properties, such as surface charge (Hagiwara & Takahashi, 1967), may be the basis for different activation level of outward rectifying K conductance in tunicate and starfish eggs.

The authors wish to express their indebtedness to Dr K. Takahashi for his valuable advice in experiments and in preparing the manuscript. They are indebted to Professor J. G. Nicholls, Drs H. Koike, Y. Kidokoro and P. B. Sargent for their kind help in preparing the manuscript. Their thanks are also due to Dr H. Kanatani and his collaborators for the guidance of preparing materials. This work was supported by the grant of the Japanese Educational Ministry.

REFERENCES

ADRIAN, R. H. & FREYGANG, W. H. (1962). The potassium and chloride conductance of frog muscle membrane, *J. Physiol.* **163**, 61–103.

ARMSTRONG, C. M. & BINSTOCK, L. (1965). Anomalies rectification in the squid giant axon injected with tetraethylammonium chloride. *J. gen. Physiol.* **48**, 859–872.

ASHMAN, R. F., KANNO, Y. & LOEWENSTEIN, W. R. (1964). The intercellular electrical coupling at a forming membrane junction in a dividing cell. *Science, N.Y.* **145**, 604–605.

BENNETT, M.V. L. & GUNDFEST, H. (1966). Analysis of depolarizing and hyperpolarizing inactivation processes in gymnotid electroplaques. *J. gen. Physiol.* **50**, 141–169.

CARMELIET, E. (1961). Chloride ions and membrane potential of Purkinje fibres. *J. Physiol.* **156**, 375–388.

CONKLIN, E. G. (1905). Mosaic development in ascidian eggs. *J. exp. Zool.* **2**, 145–223.

FATT, P. & GINSBORG, B. L. (1958). The ionic requirements for the production of action potentials in crustacean muscle fibres. *J. Physiol.* **142**, 516–543.

GEDULDIG, D. & JUNGE, D. (1968). Sodium and calcium components of action potentials in the *Aplysia* giant neurone. *J. Physiol.* **199**, 347–365.

GRUNDFEST, H. (1961). Ionic mechanisms in electrogenesis. *Ann. N.Y. Acad. Sci.* **94**, 405–457.

GRUNDFEST, H. (1966). Heterogeneity of excitable membrane: Electrophysiological and pharmacological evidence and some consequences. *Ann. N.Y. Acad. Sci.* **137**, 901–949.

HAGIWARA, S., KUSANO, K. & SAITO, N. (1961). Membrane changes of *Onchidium* nerve cell in potassium-rich media. *J. Physiol.* **155**, 470–489.

HAGIWARA, S. & NAKAJIMA, S. (1966). Differences in Na and Ca spikes as examined by application of tetrodotoxin, procaine, and manganese ions. *J. gen. Physiol.* **49**, 793–806.

HAGIWARA, S. & TAKAHASHI, K. (1967). Surface density of calcium ions and calcium spikes in the barnacle muscle fiber membrane. *J. gen. Physiol.* **50**, 583–601.

HAGIWARA, S. & TAKAHASHI, K. (1974). The anomalous rectification and cation selectivity membrane of a starfish egg cell. *J. membrane Biol.* **18**, 61–80.

HALL, A. E., HUTTER, O. F. & NOBLE, D. (1963). Current–voltage relations of Purkinje fibres in sodium-deficient solutions. *J. Physiol.* **166**, 225–240.

HALL, A. E. & NOBLE, D. (1963). The effect of potassium on the repolarizing current in cardiac muscle. *J. Physiol.* **167**, 53–54*P*.

HILLE, B. (1967). The selective inhibition of delayed potassium currents in nerve by tetraethylammonium ion. *J. gen. Physiol.* **50**, 1287–1302.

HODGKIN, A. L. & HOROWICZ, P. (1959). The influence of potassium and chloride ions on the membrane potentials of single muscle fibres. *J. Physiol.* **148**, 127–160.

HUTTER, O. F. & NOBLE, D. (1960). Rectifying properties of cardiac muscle. *Nature, Lond.* **188**, 495.

ITO, S. & YOSHIOKA, K. (1972). Real activation potential observed in sea urchin egg during fertilization. *Expl Cell Res.* **72**, 547–551.

ITO, S. & YOSHIOKA, K. (1973). Effect of various ionic compositions upon the membrane potentials during activation of sea urchin eggs. *Expl Cell Res.* **78**, 191–200.

KANATANI, H. (1969). Induction of spawning and oocyte maturation by 1-methyladenine in starfishes. *Expl Cell Res.* **57**, 333–337.

KANATANI, H., SHIRAI, H., NAKANISHI, K. & KUROKAWA, T. (1969). Isolation and identification of meiosis inducing substance in starfish *Asterias amurensis*. *Nature, Lond.* **221**, 273–274.

KATZ, B. (1949). Les constance électriques de la membrane du muscle. *Archs Sci. physiol.* **3**, 285–300.

MAENO, T. (1959). Electrical characteristics and activation potential of *Bufo* eggs. *J. gen. Physiol.* **43**, 139–157.

MIYAZAKI, S., OHMORI, H. & SASAKI, S. (1975). Action potential and non-linear current–voltage relation in starfish oocytes. *J. Physiol.* **246**, 37–54.

MIYAZAKI, S., TAKAHASHI, K. & TSUDA, K. (1972). Calcium and sodium contributions to regenerative responses in the embryonic excitable cell membrane. *Science, N.Y.* **176**, 1441–1443.

MIYAZAKI, S., TAKAHASHI, K. & TSUDA, K. (1974*a*). Electrical excitability in the egg cell membrane of the tunicate. *J. Physiol.* **238**, 37–54.

MIYAZAKI, S., TAKAHASHI, K., TSUDA, K. & YOSHII, K. (1974*b*). Analysis of non-linearity observed in the *I–V* relation of the tunicate embryo. *J. Physiol.* **238**, 55–77.

MORRILL, G. A., ROSENTHAL, J. & WATSON, D. E. (1966). Membrane permeability changes in amphibian eggs at ovulation. *J. cell. Physiol.* **67**, 375–382.

NAKAJIMA, S. (1966). Analysis of K inactivation and TEA action in the supramedullary cells of puffer. *J. gen. Physiol.* **49**, 629–640.

NAKAJIMA, S., IWASAKI, S. & OBATA, K. (1962). Delayed rectification and anomalous rectification in frog's skeletal muscle membrane. *J. gen. Physiol.* **46**, 97–115.

NAKAJIMA, S. & KUSANO, K. (1966). Behavior of delayed current under voltage clamp in the supramedullary neurons of puffer. *J. gen. Physiol.* **49**, 613–628.

NAKAMURA, Y., NAKAJIMA, S. & GRUNDFEST, H. (1965). Analysis of spike electrogenesis and depolarizing K inactivation in electroplaques of *Electrophorus electricus*, L. *J. gen. Physiol.* **49**, 321–349.

NOBLE, D. (1965). Electrical properties of cardiac muscle attributable to inward-going (anomalous) rectification. *J. cell. comp. Physiol.* **66**, suppl. 2, 127–136.

REUBEN, J. P., WERAMAN, R. & GRUNDFEST, H. (1961). The ionic mechanisms of hyperpolarizing responses in lobster muscle fibers. *J. gen. Physiol.* **45**, 243–265.

STEINHARDT, R. A., LUNDIN, L. & MAZIA, D. (1971). Bioelectric responses of the echinoderm egg to fertilization. *Proc. natn. Acad. Sci. U.S.A.* **68**, 2426–2430.

STEINHARDT, R. A., SHEN, S. & MAZIA, D. (1972). Membrane potential, membrane resistance and an energy requirement for the development of potassium conductance in the fertilization reaction of echinoderm egg. *Expl Cell Res.* **72**, 195–203.

TAKAHASHI, K., MIYAZAKI, S. & KIDOKORO, Y. (1971). Development of excitability in embryonic muscle cell membranes in certain tunicates. *Science, N.Y.* **171**, 415–418.

TASAKI, I. & HAGIWARA, S. (1957). Demonstration of two stable potential states in the squid giant axon under tetraethylammonium chloride. *J. gen. Physiol.* **40**, 859–885.

TRAUTWEIN, W. & KASSEBAUM, D. G. (1961). On the mechanism of spontaneous impulse generation in the pacemaker of the heart. *J. gen. Physiol.* **45**, 317–330.

TUPPER, J., SAUNDERS, J. W., JR. & EDWARDS, C. (1970). The onset of electrical coupling between cells in the developing starfish embryo. *J. cell Biol.* **46**, 187–190.

TYLER, A., MONROY, A., KAO, C. Y. & GRUNDFEST, H. (1956). Membrane potential and resistance of the starfish egg before and after fertilization. *Biol. Bull. mar. biol. Lab., Woods Hole* **111**, 153–177.